Journal of Thermal Analysis, Vol. 37 (1991) 1161-1177

Dedicated to Professor Dr. H. J. Seifert on the occasion of his 60th birthday

A KINETIC ANALYSIS OF THE PYROLYSIS OF SOME AUSTRALIAN COALS BY NON-ISOTHERMAL THERMOGRAVIMETRY

S. Ma[a], *J. O. Hill*[a] *and S. Heng*[b]

[a]DEPARTMENT OF CHEMISTRY, LA TROBE UNIVERSITY, BUNDOORA, VICTORIA 3083, AUSTRALIA
[b]COAL CORPORATION OF VICTORIA, RESEARCH FACILITY; GIPPSLAND INSTITUTE OF ADVANCED EDUCATION, CHURCHILL, VICTORIA 3842, AUSTRALIA

(Received June 15, 1990)

The pyrolysis of a suite of brown coal samples and bituminous coal maceral concentrates is investigated by non-isothermal thermogravimetry. The TG data for these coals reveal a two-stage pyrolysis process. The activation energy for the primary pyrolysis stage is considerably higher than that for the secondary pyrolysis stage. It is evident that a particular coal may be characterised by the weighted mean apparent pyrolysis activation energy which correlates with the corresponding specific energy of the coal.

Pyrolysis is a fundamental process in the combustion, carbonization and gasification of coal. The study of pyrolysis kinetics is essential for the understanding of the mechanism and mathematical modelling of the pyrolysis process which may lead to improved techniques for coal conversion. In addition, as pyrolysis is directly related to the chemical composition of coal, the related kinetic parameters derived from thermal analysis can also be used for coal characterization.

Both thermogravimetry and differential thermal analysis have been applied to determine the kinetics of coal decomposition [1]. Generally, TG is the preferred method for such determinations since the relevant mass changes are easier to measure than the associated heat effects [2].

John Wiley & Sons, Limited, Chichester
Akadémiai Kiadó, Budapest

The kinetics of coal pyrolysis may be investigated by either isothermal or non-isothermal thermogravimetry. The non-isothermal method has some advantages over the traditional isothermal analysis [3–10].

In the present study, the non–isothermal TG data, obtained for the pyrolysis of three brown coals and four bituminous coals from Australia are used to derive the corresponding pyrolysis kinetic parameters, via incorporation into a computer program (KNIS) [11], which systematically attempts to match such data with several well–known, solid-state decomposition kinetic models. Further, the relationship between mean pyrolysis activation energy and coal specific energy is investigated.

Experimental

The samples investigated included three brown coal samples from Morwell, Loy Yang and Gelliondale coal fields in Victoria and four bituminous coal maceral concentrates of Bulli vitrinite, Bulli inertinite, Liddell vitrinite, and Liddell inertinite from New South Wales. The bituminous coal maceral concentrates were hand picked from 'run-of-mine' lump coal samples. The chemical analysis data for all samples investigated are shown in Table 1. Simultaneous TG and DTG curves were obtained using a Rigaku–Denki, Type 8085 (Thermoflex) TG–DTA Thermal Analysis System using the following experimental conditions: atmosphere: nitrogen; flow rate: 0.1 $dm^3 \cdot min^{-1}$; sample size: 15 mg; heating rate: 10 $deg \cdot min^{-1}$; temperature range: 20 to 950°; crucible: platinum; TG range: 10 mg; DTG range: 5 $mg \cdot min^{-1}$. All samples were air dried and pulverized to pass an 80 mesh sieve.

Results and discussion

The TG and DTG curves for the Morwell brown coal samples are shown in Fig. 1. The mass loss below 200° is related to the removal of moisture. The subsequent pyrolysis process includes two stages [12], the primary and secondary pyrolysis stages, as revealed by a corresponding DTG peak around 400° and a poorly resolved shoulder to the right side of this main peak. The TG curves of all the coal samples investigated in the present study are shown in Fig. 2. The DTG curves of Victorian brown coal samples, Bulli bituminous coal maceral concentrates and Liddell bituminous coal maceral

Table 1 Chemical analysis of coal samples

Sample	Morwell	Gelliondale	Loy Yang	Bulli vitrinite	Bulli inertinite	Liddell vitrinite	Liddell inertinite
Proximate analysis							
Moisture, (%)	12.7	7.3	15.6	1.6	1.5	6.3	2.9
Ash, (%db)[a]	3.8	5.4	1.1	1.4	13.6	1.4	9.4
M&I, (%db)[b]	2.3	3.0	0.8	–	–	–	–
VM, (%db)[c]	47.7	49.9	51.7	22.3	15.6	35.2	31.1
FC[d]	48.5	44.7	47.2	76.3	70.8	63.4	59.5
Specific energy							
Q_g (dry, $MJ \cdot Kg^{-1}$)	26.21	25.99	26.16	35.7	30.3	33.7	30.8
Ultimate analysis, (% daf)[e]							
Carbon	70.2	68.2	68.4	88.4	87.7	81.8	82.7
Hydrogen	4.8	4.8	4.9	5.3	4.6	5.5	5.6
Nitrogen	0.55	0.57	0.57	2.0	1.6	2.1	2.2
Sulphur	0.27	0.80	0.32	0.3	0.3	0.4	0.4
Oxygen (diff.)[f]	24.2	25.6	25.8	4.0	5.8	10.2	9.1
H/C Atom. ratio	0.820	0.844	0.860	0.719	0.629	0.807	0.813
O/C Atom. ratio	0.259	0.282	0.283	0.034	0.050	0.093	0.082

[a] db = dry basis, [b] Minerals and inorganics, [c] Volatile matter, [d] Fixed carbon, [e] daf = dry and ash free, [f] diff = by difference

concentrates are shown in Figs 3 to 5 respectively. Some characteristics of pyrolysis are listed in Table 2. The initial pyrolysis temperature T_i is taken as the onset temperature of the corresponding initial mass loss. T_m is the temperature at which the maximum rate R_m of volatilization occurs. The moisture content M is the mass loss below 200°, and the final volatile matter released corresponds to the mass loss between 200 and 950°.

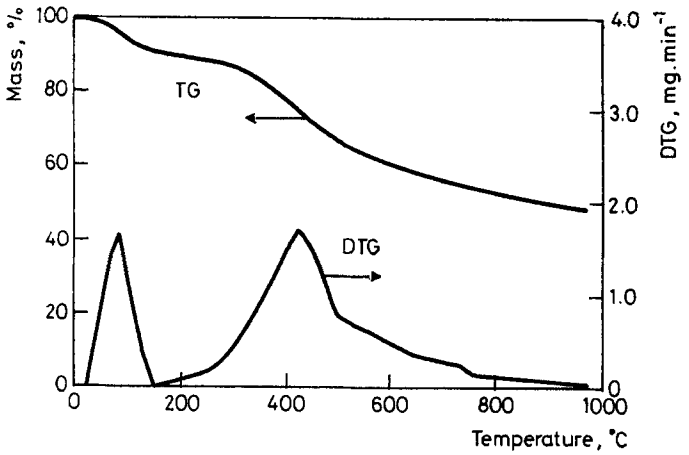

Fig. 1 TG and DTG curves for Morwell coal pyrolysis ($10°C \cdot min^{-1}$)

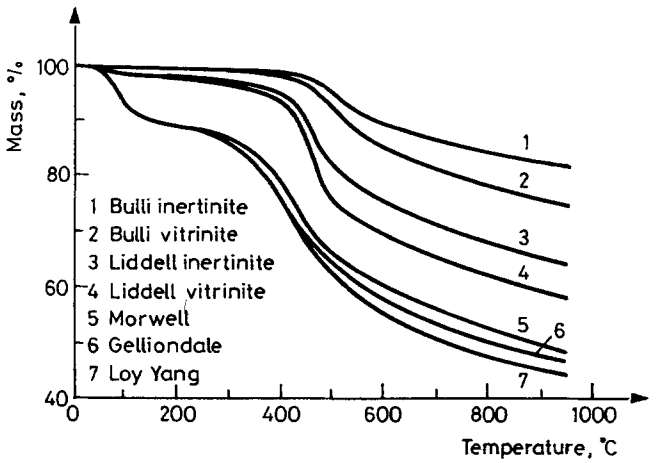

Fig. 2 TG curves for the pyrolysis of Australian coal samples

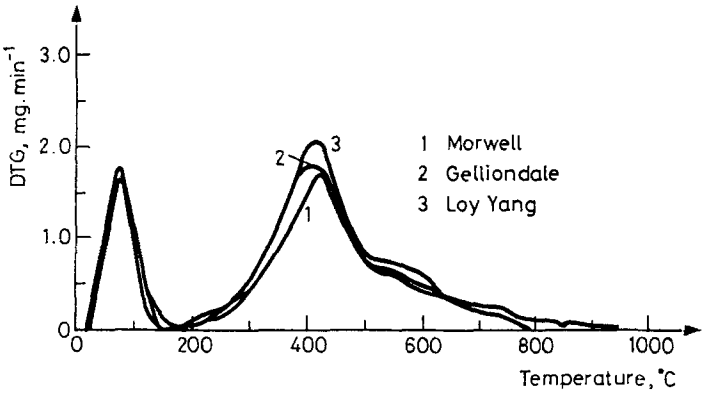

Fig. 3 DTG curves of brown coal samples

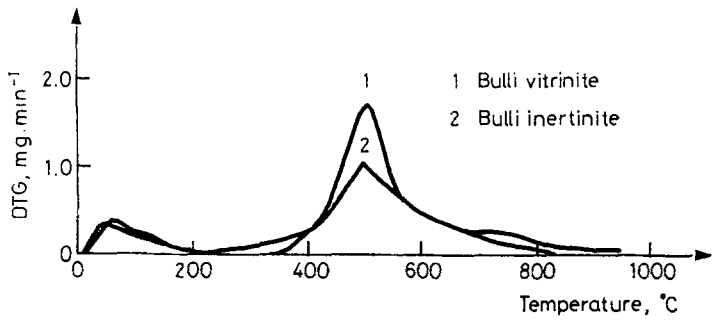

Fig. 4 DTG curves of Bulli bituminous coal samples

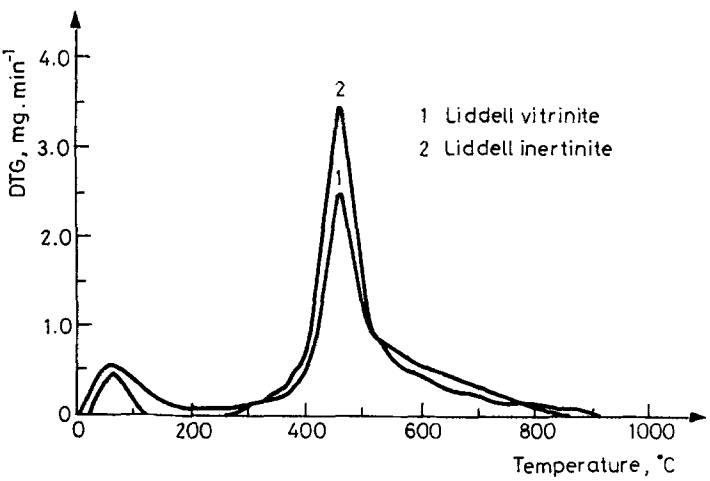

Fig. 5 DTG curves of Liddell bituminous coal samples

Table 2 Pyrolysis characteristics of coal samples

Sample	Moisture, , %(ad)[a]	Volatile matter %(db)[b]	T_i, °C	T_m, °C	R_m, %·min^{-1}
Morwell	10.4	45.4	324	425	1.73
Gelliondale	10.9	46.8	315	405	1.82
Loy Yang	10.7	50.3	316	417	2.05
Bulli vitrinite	1.5	22.7	435	496	1.71
Bulli inertinite	0.2	18.1	424	497	1.07
Liddell vitrinite	2.7	40.2	401	454	3.46
Liddell inertinite	2.1	34.3	401	455	2.52

[a] (air dried), [b] (dry basis)

The moisture content and volatile matter of low rank brown coal samples used in this study are higher those that of the bituminous coal samples. The pyrolysis of low rank coal commences at a lower temperature compared to bituminous coal. The Bulli and Liddell coals show significantly different thermal properties with the Bulli coal associated with higher T_i and T_m values and a lower R_m than Liddell coal. There is no significant difference in the T_i and T_m parameters between the vitrinite and inertinite macerals for both Bulli and Liddell coals. However, the Liddell vitrinite and inertinite have higher volatile matter contents than the corresponding Bulli vitrinite and inertinite concentrates. For both the Bulli and Liddell coals, the inertinite maceral has a lower volatile matter content and a lower maximum volatilization rate R_m than the vitrinite maceral. The maximum rates of volatilization for the Liddell Coal samples are substantially higher than those of brown coals.

Prior to a discussion of the kinetic data obtained, as related to the pyrolysis of these coal samples, it is necessary to review the theoretical premise on which the analysis procedure is based. For the thermal decomposition of a solid, the relevant kinetic Eq. [13] is

$$\frac{d\alpha}{dt} = k \cdot f(\alpha) \tag{1}$$

where α is the degree of conversion, k is the temperature dependent rate constant, and $f(\alpha)$ depends on the particular decomposition mechanism. At a constant heating rate β, $\beta = dT/dt$, and according to Arrhenius,

$$k = A \exp(-E/RT) \tag{2}$$

where A is pre-exponential factor, and E is the activation energy. Thus Eq. (1) becomes

$$\frac{d\alpha}{dt} = \frac{A}{\beta} \cdot f(\alpha) \cdot \exp(-E/RT) \tag{3}$$

An integrated form of Eq. (3) may be approximately expressed by [6]:

$$\log\left[\frac{F(\alpha)}{T^2}\right] = \log\left[\frac{AR}{\beta(E + 2RT)}\right] - \frac{E}{2.303RT} \tag{4}$$

If it is assumed that $(E + 2RT)$ is a constant, which is valid for a high activation energy and a moderate temperature [6], a plot of $\log[F(\alpha)/T^2]$ against $1/T$ should result in a straight line with a slope of $-E/2.303R$ for the correct form of $F(\alpha)$. Several kinetic models have been proposed and these are listed in Table 3, together with the form of $f(\alpha)$ and $F(\alpha)$ used. The KNIS program [11] incorporates all of these models and attempts to match a given set of TG data with each model systematically. The model associated with the 'best fit' of such data with Eq. (4), hence specifies the mechanism and yields the relevant kinetic parameters.

In terms of coal pyrolysis, it is necessary to provide some preliminary interpretation of the activation energies obtained from such a data analysis procedure. Coal pyrolysis is a complex process and involves a range of chemical and physical processes including the breaking of chemical bonds and associated molecular rearrangements, heat transfer between atmosphere and sample and the transport of volatile matter from the interior of the coal to the surface. All these concurrent processes contribute to the overall empirical mass loss. Thus, the kinetic parameters derived from the relevant TG curve should be considered as apparent values which are not precisely related to any one particular mechanistic step.

Cumming [14] ranked the reactivities of coals by utilizing the concept of a weighted mean apparent activation energy (E_m), as defined in the equation:

$$E_m = F_1E_1 + F_2E_2 + \ldots + F_nE_n \tag{5}$$

Table 3 Kinetic models incorporated into the KNIS program

Model	Symbol	$f(\alpha)$	$F(\alpha)$
Coats–Redfern[a]	*C*	$(1-\alpha)^n$	$[1-(1-\alpha)^{1-n}]/(1-n)$
Nucleation and nuclei growth[b]			
Mampel unimolecular law	*A1*	$1-\alpha$	$-\ln(1-\alpha)$
Two–dimensional growth	*A2*	$2(1-\alpha)[-\ln(1-\alpha)]^{1/2}$	$[-\ln(1-\alpha)]^{1/2}$
Three–dimensional growth	*A3*	$3(1-\alpha)[-\ln(1-\alpha)]^{2/3}$	$[-\ln(1-\alpha)]^{1/3}$
Prout–Thompkins branching nuclei	*A4*	$\alpha(1-\alpha)$	$\ln[\alpha/(1-\alpha)]$
Diffusion[b]			
Parabolic law	*D1*	$\alpha-1$	$\alpha^2/2$
Valensi equation	*D2*	$[-\ln(1-\alpha)]^{-1}$	$(1-\alpha)\ln(1-\alpha)+\alpha$
Jander equation	*D3*	$3(1-\alpha)^{1/3}/2[(1-\alpha)^{-1/3}-1]$	$[1-(1-\alpha)^{1/3}]^2$
Brounshtein–Ginstling equation	*D4*	$3/2[(1-\alpha)^{-1/3}-1]$	$1-2/3\alpha-(1-\alpha)^{2/3}$
Phase boundary movement[b]			
One–dimensional	*R1*	constant	α
Two–dimensional	*R2*	$2(1-\alpha)^{1/2}$	$1-(1-\alpha)^{1/2}$
Three–dimensional	*R3*	$3(1-\alpha)^{2/3}$	$1-(1-\alpha)^{1/3}$

[a] A. W. Coats and J. P. Redfern, Nature, 201(1964) 68.

[b] J. Šestak and G. Berggren, Thermochim. Acta, 3(1971) 1.

where F_1 to F_n are the weighted fractions, and E_1 to E_n are the individual apparent activation energies, as related to corresponding regions of Arrhenius linearity for the pyrolysis processes. This procedure for expressing activation energies for coal pyrolysis processes, has been adopted in the present work.

For the various coals studied, the relevant kinetic parameters, obtained via application of the TG data analysis procedures previously described, are given in Table 4. These parameters are calculated in terms of the 3-dimensional diffusion model D_3, as expressed by the Jander equation [15, 16]. For each sample, the apparent activation energy E_m and pre-exponential factor A, as related to the pyrolysis process, relate to a corresponding α factor in the range 0.03 to 0.95. The 'best fit' criterion with model D_3 is consistent with a correlation coefficient $R_f > 0.99$.

Fundamentally, these coals exhibit two pyrolysis stages and two regions of linearity with respect to Arrhenius kinetic plots. Such behaviour has been found previously by Smith *et al.* [17] for several coals.

In the primary pyrolysis stage below 500°, the volatile matter evolved is mainly methane and corresponding homologues, unsaturated hydrocarbons, and CO, CO_2, H_2O due to the decomposition of the substituted groups and the inherent aliphatic (or hydroaromatic) structures. [12, 18, 19] The maximum rate of mass loss occurs in this stage and the corresponding activation energy is also greater than that for the secondary pyrolysis stage. In the primary pyrolysis stage, brown coal has a comparatively low activation energy, as compared with the bituminous coals. This is probably related to the high oxygen content of brown coal, since oxygen containing functional groups, such as carboxylic acid and carboxylate are liable to decompose at low temperatures. The three brown coal samples used in this study have similar kinetic parameters, with Loy Yang coal having the highest activation energy.

For the bituminous coal macerals, the vitrinite concentrates have a higher activation energy in the primary stage than the inertinite concentrates. This is associated with the higher maximum rate of volatilization for the vitrinite macerals. Similar results are obtained for the pyrolysis of some Chinese coal macerals as published by Pang and Dai. [9] From their results, the order of activation energy is established as vitrinite>inertinite>fusinite.

For the same maceral concentrates, the samples from the Liddell coal field have a lower activation energy and frequency factor than the corresponding Bulli maceral samples.

Table 4 Kinetic parameters for coal pyrolysis ($10^{\circ}C \cdot min^{-1}$)[a]

Sample	Temp. range, °C	F^b	E, $kJ \cdot mol^{-1}$	A, s^{-1}	r	E_m, $kJ \cdot mol^{-1}$
Morwell	278–474	0.476	79.67	$6.80 \cdot 10^{1}$	0.9992	46.41[c]
	474–830	0.403	21.06	$2.08 \cdot 10^{-3}$	0.9988	
Gelliondale	266–451	0.460	84.27	$2.16 \cdot 10^{2}$	0.9995	47.43
	451–840	0.440	19.69	$1.79 \cdot 10^{-3}$	0.9994	
Loy Yang	249–453	0.478	80.49	$1.06 \cdot 10^{2}$	0.9994	47.31
	453–848	0.437	20.18	$2.03 \cdot 10^{-3}$	0.9955	
Bulli vitrinite	390–518	0.416	168.56	$2.87 \cdot 10^{7}$	0.9990	83.47
	518–880	0.482	27.79	$4.24 \cdot 10^{-3}$	0.9966	
Bulli inertinite	360–554	0.435	116.91	$3.50 \cdot 10^{3}$	0.9932	67.52
	554–897	0.471	35.38	$1.02 \cdot 10^{-2}$	0.9985	
Liddell inertinite	360–505	0.511	143.24	$1.65 \cdot 10^{6}$	0.9916	80.15
	505–880	0.377	18.47	$1.36 \cdot 10^{-3}$	0.9969	
Liddell inertinite	309–529	0.530	111.01	$4.67 \cdot 10^{3}$	0.9900	67.77
	529–872	0.381	23.49	$2.60 \cdot 10^{-3}$	0.9982	

[a] Calculated using the 3-dimensional diffusion model $D3$

[b] weighed fraction

[c] Em (Specimen calculation) $= 79.67 \cdot 0.476 + 21.06 \cdot 0.403 = 46.41$ $kJ \cdot mol^{-1}$

In the secondary pyrolysis stage, which occurs at higher temperatures, bond breaking and structural rearrangements occur [19]. In this process, the release of hydrogen dominates [12, 18, 19] and some CO, CS_2 and HCN are also released. The activation energy in this stage is lower than that of the primary stage and appears to be independent of the coal rank. Generally, the mass transfer process has a low activation energy [17, 20] and hence, the secondary stage at higher temperature is mainly a diffusion process.

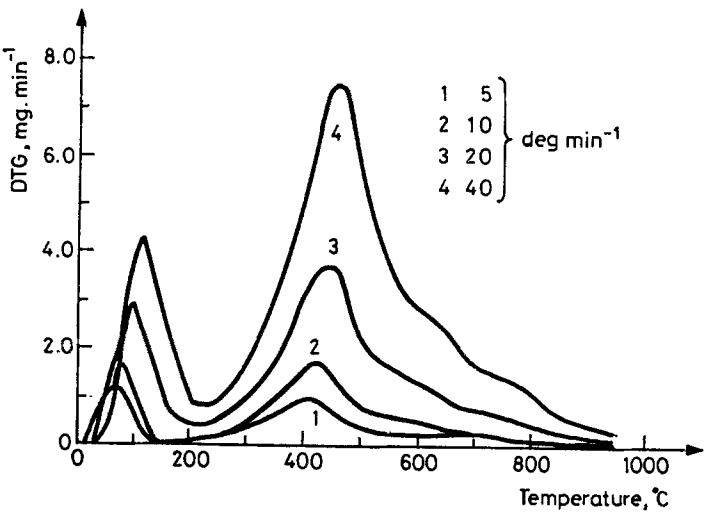

Fig. 6 DTG curves of Morwell coal samples at different heating rates

It is well known that heating rate has an effect on coal pyrolysis. The pyrolysis of Morwell brown coal was investigated using different heating rates, ranging from 5 to 40 deg·min^{-1}. The DTG profiles obtained are shown in Fig. 6 and the pyrolysis characteristics are listed in Table 5. The initial pyrolysis temperature T_i and the temperature of maximum pyrolysis rate T_m are found to increase with increasing heating rate. The maximum rate of volatile matter release increases linearly with increasing heating rate (Fig. 7) while the moisture content and volatile matter released appear to be independent of heating rate.

The kinetic parameters of Morwell coal at different heating rates are shown in Table 6. The average E_m is 46.8±2.8 kJ·mol^{-1} irrespective of heating rate. It appears that the weighted mean apparent activation energy increases slightly with increasing heating rate.

The activation energies for the first pyrolysis stage, as reported in Table 4 arein the range 80–84 $kJ \cdot mol^{-1}$ for the brown coal samples and 111-168 $kJ \cdot mol^{-1}$ for bituminous coals, and the weighted mean apparent activation energies E_m are in the range 46–84 $kJ \cdot mol^{-1}$. These values are comparable with some literature data. From thermogravimetric data of a sub–bituminous coal decomposition over the temperature range 523-923 K, Serageldin *et al.* [1] obtained an activation energy of 50 $kJ \cdot mol^{-1}$ by the Arrhenius method. Ko *et al.* [21] applied a first–order single-reaction model for coal devolatilization over a wide range of heating rates ($0.1–10^4$ $°C \cdot s^{-1}$) and obtained E = 27–44 $kJ \cdot mol^{-1}$. Guo *et al.* [22] investigated the pyrolysis of ten Chinese lignites and these yielded E = 55–160 $kJ \cdot mol^{-1}$ by the Coats–Redfern method.

Table 5 Pyrolysis characterestics of Morwell brown coal at different heating rates

Heating rate $°C \cdot min^{-1}$	Moiture % (ad)	Volatile matter % (db)	T_i, °C	T_m, °C	R_m, $\% \cdot min^{-1}$
5	10.0	45.2	316	412	0.97
10	10.4	45.4	324	425	1.73
20	10.2	44.4	334	440	3.72
40	9.9	43.4	360	451	7.47

Table 6 The kinetic parameters for Morwell coal pyrolysis at different heating rates

Heating rates $°C \cdot min^{-1}$	Temp. range, °C	E, $kJ \cdot mol^{-1}$	A, s–1	r	E_m, $kJ \cdot mol^{-1}$
5	240–443	78.02	$2.74 \cdot 10^1$	0.9972	44.00
	457–875	23.21	$1.23 \cdot 10^{-3}$	0.9969	
10	278–474	79.67	$6.80 \cdot 10^1$	0.9992	46.41
	474–830	21.06	$2.08 \cdot 10^{-3}$	0.9988	
20	259–488	78.18	$8.93 \cdot 10^1$	0.9990	48.03
	488–837	22.34	$5.19 \cdot 10^{-3}$	0.9976	
40	287–498	80.15	$1.72 \cdot 10^2$	0.9977	48.73
	498–856	25.73	$1.41 \cdot 10^{-2}$	0.9925	

It should be noted that the Kissinger analysis procedure [23], based on the maximum rate temperature, is also used in the analysis of coal pyrolysis data [24–26]. The Kissinger analysis can be expressed as:

$$\ln\left(\frac{\beta}{T_{max}^2}\right) = \ln\left(\frac{RT}{E}\right) - \frac{E}{RT_{max}} \tag{6}$$

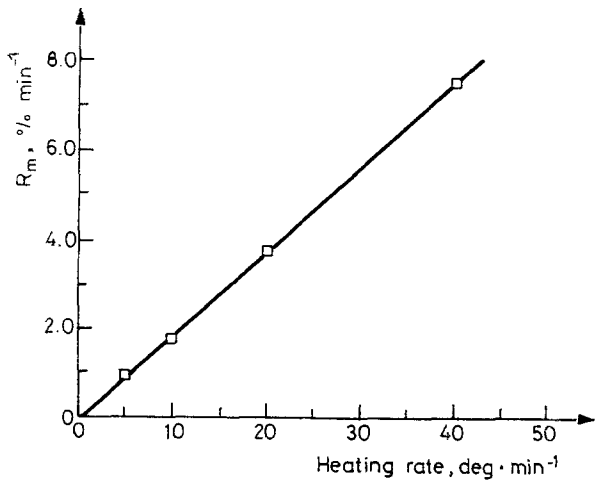

Fig. 7 The maximum rate of pyrolysis of Morwell coal at different heating rates

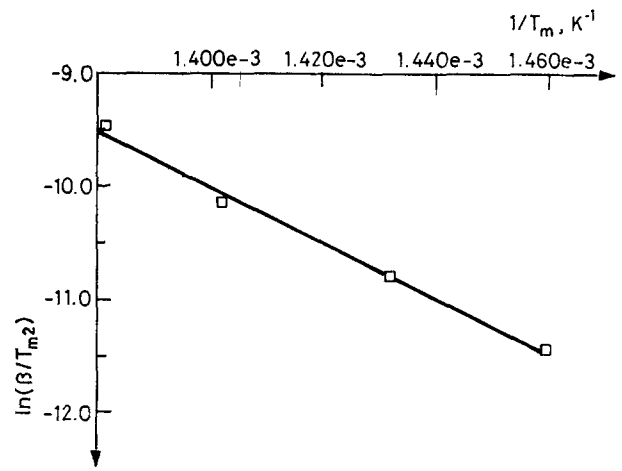

Fig. 8 The kinetic analysis of TG data for Morwell brown coal by the Kissinger procedure

The relevant $f(\alpha) = (1-\alpha)^n$. This method is only valid for a narrow temperature range around the maximum temperature ($0.9–1.1T_m$) [27].

The Kissinger analysis procedure is applied here for Morwell coal and the corresponding kinetic plot is shown in Fig. 8. The relevant kinetic parameters are $E = 203.94$ kJ·mol^{-1} and $A = 1.628 \cdot 10^{13}$ s^{-1}. These values are close to the literature values derived from the Kissinger equation [25, 28]. Elder *et al.* [25] investigated the thermal characteristics of six Kentucky bituminous coals undergoing pyrolysis in an inert atmosphere, and obtained $E = 198–220$ kJ·mol^{-1} and $A = 2\text{-}85 \cdot 10^{12}$ s^{-1} for the major mass loss region by using a modified Kissinger equation and the T_m parameter. Brown [28] employed the Kissinger equation to calculate kinetic parameters for some Australian coals and obtained $E = 186.2$ kJ·mol^{-1}.

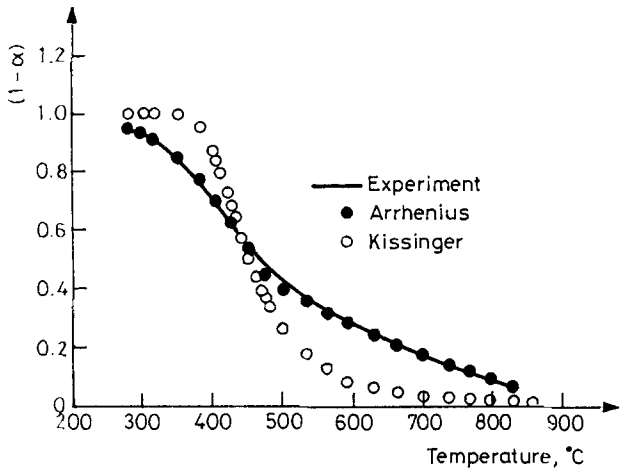

Fig. 9 Comparison of Arrhenius, Kissinger and Experimental ($1–\alpha$) functions for the pyrolysis of Morwell brown coal

However, a comparison of the experimental data for the Morwell coal at 10 deg·min^{-1} and that calculated by Arrhenius and Kissinger analyses shows (Fig. 9) that the kinetic parameters derived from an Arrhenius analysis yield a good curve fit over the entire temperature range, whereas the kinetic parameters derived from a Kissinger analysis curve fit only within a very narrow range around the maximum rate temperature. This is also demonstrated by the study of Elder [26, 29] on the thermal degradation of West Kentucky bituminous coals. In general, the Kissinger analysis produces higher values of kinetic parameters than the Arrhenius analysis procedure. Gadalla [27] has applied various methods, including the Arrhenius and Kissinger analysis

procedures, to the kinetics of the dissociation of hydrated calcium and magnesium oxalates. Their results show that the Kissinger method is not suitable for application to reactions occurring over wide temperature ranges or when the activation energy and pre-exponential factor vary over a wide range.

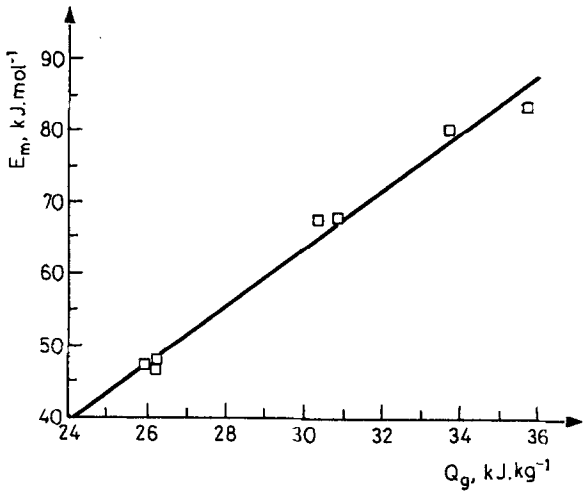

Fig. 10 Relationship between E_m and Q_g for various coal samples

Figure 10 shows the relationship between the E_m and specific energy of the coal samples investigated. The correlation can be expressed as a straight line:

$$E_m\ (\text{kJ}\cdot\text{mol}^{-1}) = 4.03Q_g\ (\text{MJ}\cdot\text{kg}^{-1}) - 57.48 \qquad (7)$$

with a correlation coefficient $r = 0.992$. Thus, the higher the reactivity, the lower is the specific energy. It is also apparent from Table 4 that the values of Em for brown coals are much lower than those for bituminous coals. In the ASTM system, the specific energy is used in the classification of coals of rank lower than medium volatile bituminous [30]. Based on this work, it is suggested that the Em value is an indicator of reactivity, not only in the case of the burning process [14], but also in the pyrolysis process of coals.

In summary, from the results obtained for a suite of brown coals and bituminous coal maceral concentrates, the three-dimensional diffusion integral kinetics model is valid for the overall coal pyrolysis process. The kinetic plot clearly shows the two stages of pyrolysis. The activation energy obtained for brown coal is in the range of 80 to 84 kJ·mol^{-1} for the primary

pyrolysis, and 19 to 21 $kJ \cdot mol^{-1}$ for the secondary pyrolysis. The bituminous coals have lower volatile matter content, higher initial pyrolysis temperature, higher activation energies and frequency factors than the corresponding parameters for brown coals. The activation energies of the bituminous coals are 111-168 and 18-35 $kJ \cdot mol^{-1}$ for the primary stage and the secondary stage respectively. For all the coal samples investigated, the secondary pyrolysis has a much lower activation energy than the primary pyrolysis, which suggests that the primary pyrolysis is dominated by chemical decomposition processes, whereas the secondary pyrolysis process is dominated by mass and heat transfer processes. The behavior of coals may be characterised by the weighted mean apparent activation energy E_m. A correlation between E_m and specific energy of coals was also found.

References

1 M. A. Serageldin and W. Pan, Amer. Chem. Soc. Div. Fuel Chem., 29 (1984) 112.
2 S. Ma, J. O. Hill and S. Heng, J. Thermal Anal., 35 (1989) 977.
3 W. W. Wendlandt, 'Thermal Analysis', Wiley-Interscience, New York 1986, p. 59.
4 J. P. Elder, J. Thermal Anal., 30 (1985) 657.
5 K. Rajeshwar, Thermochim. Acta, 45 (1981) 253.
6 T. V. Lee and S. R. Beck, Amer. Ind. Chem. Eng. J., 30 (1984) 517.
7 J. M. Vargas and D. D. Perimutter, Ind. Eng. Chem. Process Des. Dev., 25 (1986) 49.
8 W. Wanzl, Fuel Processing Tech., 20 (1988) 317.
9 B. Pang and H. Dai, J. Fuel Chem. Tech., 17 (1989) 1.
10 S. Guo, Q. Yuan, and S. Zhu, J. Fuel Chem. Tech., 17 (1989) 55.
11 S. Ma, G. Huang and J. O. Hill, Thermochim. Acta, (1991) in press.
12 M. I. Pope and M. D. Judd, 'Differential Thermal Analysis', Heyden, London 1977, p. 116.
13 J. Šestak and G. Berggren, Thermochim. Acta, 3 (1971) 1.
14 J. W. Cumming, Fuel, 63 (1984) 436.
15 W. Jander, Z. Anorg. Allgem. Chem., 163 (1927) 1.
16 P. G. Shewmon, 'Diffusion in Solids', McGraw-Hill, New York 1963.
17 S. E. Smith, R. C. Neavel, E. J. Hippo and R. N. Miller, Fuel, 60 (1981) 458.
18 J. Chen and X. Sun, J. Eng. Thermophysics, 7 (1986) 172.
19 'Chemistry of Coal Conversion' R. H. Schlosberg, Ed., Plenum Press, New York 1985, p. 123.
20 M. R. Khan, Fuel, 66 (1987) 1626.
21 C. H. Ko, D. M. Sanchez, W. A. Peters and J. B. Howard., Am. Chem. Soc. Div. Fuel Chem., 32 (1988) 112.
22 S. Guo, Q. Yuan and S. Zhu, J. Fuel Chem. and Tech., 17 (1989) 55.
23 H. E. Kissinger, J. Res. Natl. Bur. Stand., 57 (1957) 712.
24 P. Hanaba, H. Juntgen and W. Peters, Brennst. Chem., 49 (1989) 368.
25 J. P. Elder and M. B. Harris, Fuel, 63 (1984) 262.
26 J. P. Elder and V. B. Reddy, Reactivity of Solids, 2 (1987) 337.
27 A. M. M. Gadalla, Thermochim. Acta, 74 (1984) 255.
28 H. R. Brown, J. Inst. Fuel, 30 (1957) 137.
29 J. P. Elder, Thermochim. Acta, 95 (1985) 41.
30 P. H. Given and R. F. Yarzab, 'Analytical Methods for Coal and Coal Products', C. Karr, Jr. Ed., Academic Press, New York 1978, p. 27.

Zusammenfassung — Mittels nichtisothermer Thermogravimetrie wurde die Pyrolyse einer Reihe von Braunkohlenproben und Mazeralkonzentrate aus bituminösen Kohlen untersucht. Die TG-Daten dieser Kohlen weisen einen zweischrittigen Pyrolyseprozeß auf. Die Aktivierungsenergie für den ersten Pyrolyseschritt ist erheblich höher als die des zweiten Pyrolyseschrittes. Es ist offensichtlich, daß eine gegebene Kohle durch den gewichteten Mittelwert der scheinbaren Aktivierungsenergie der Pyrolyse charakterisiert werden kann, welcher mit der entsprechenden spezifischen Energie der Kohle korreliert.